Dielectric, ferroelectric properties, and grain growth of $Ca_xBa_{1-x}Nb_2O_6$ ceramics with tungsten-bronzes structure

Shanming Ke,[1,2,a)] Huiqing Fan,[1,b)] Haitao Huang,[2,b)] H. L. W. Chan,[2] and Shuhui Yu[3]
[1]*State Key Laboratory of Solidification Processing, School of Materials Science, Northwestern Polytechnical University, Xi'an 710072, People's Republic of China*
[2]*Department of Applied Physics and Materials Research Center, The Hong Kong Polytechnic University, Hung Hom, Kowloon, Hong Kong*
[3]*Shenzhen Institute of Advanced Technology, Chinese Academy of Sciences, Shenzhen 518067, People's Republic of China*

(Received 26 March 2008; accepted 10 May 2008; published online 17 July 2008)

Dielectric properties, microstructures, and phase transition behaviors of α and β phases of $CaxBa_{1-x}Nb_2O_6$ ($x=0.22$, 0.30, and 0.38) ceramics were investigated. All the three compositions had partially filled tungsten-bronze structure (TTB) and relatively high Curie temperatures (up to 345 °C) compared with $Sr_{1-x}Ba_xNb_2O_6$. The α phase exhibits unambiguously a diffused phase transition, while the β phase is associated with an incommensurate phase and needs to be further studied. The dielectric and ferroelectric properties of $Ca_xBa_{1-x}Nb_2O_6$ ceramics were strongly processing-dependent. A mechanism was proposed to explain the grain growth behavior of TTB ceramic niobates. © *2008 American Institute of Physics*. [DOI: 10.1063/1.2956615]

I. INTRODUCTION

The relaxor ferroelectrics, strontium barium niobate ($Sr_{1-x}Ba_xNb_2O_6$, abbreviated as SBN, $0.25<x<0.75$), with a structure closely related to tetragonal tungsten bronze (TTB) (*P4bm* or 4mm), are of immense importance in many technological applications such as pyroelectric detectors, spatial light modulators, electro-optic, and surface acoustic wave devices.[1–3] Recently, large single crystals of calcium barium niobate, $Ca_xBa_{1-x}Nb_2O_6$, (CBN100x) with $x=0.28$ have been successfully grown by the Czochralske method.[4,5] CBN28 also belongs to TTB structure and possesses quite similar optical properties with SBN, and it experiences much higher ferroelectric phase transition temperature (around 265 °C) than SBN61 does (around 79 °C).[4–8]

The excellent optical and ferroelectric properties of CBN28 provide potential for applications at relatively high temperatures. Song *et al.* reported that the dielectric properties of the CBN28 single crystal showed strong orientation dependence.[6] Therefore, it is worth investigating the dielectric properties of CBN polycrystalline ceramics, especially with textured microstructures. Ismailzade[9] has reported the existence of $Ca_xBa_{1-x}Nb_2O_6$ solid solution with $x=0.2–0.4$. However, information on the microstructure and physical properties of CBN with different calcium contents is rare.

Although CBN28 single crystals have been gown, little work has been conducted to study their ferroelectric and dielectric properties. Thin films of CBN28 on $SrTiO_3$ and MgO substrates were recently grown by pulsed laser deposition.[10,11] The detailed microstructure of CBN28 films and their interface structures have been investigated. To our knowledge, experimental data on CBN ceramics, single crystals, and films in the whole solid solution range are very scarce. The situation is extremely unfavorable for a complete understanding of the microstructure and its related physical properties of CBN system. Does CBN, like its counterpart SBN, exhibit a relaxor-paraelectric phase transition or a first-order normal-relaxor ferroelectric phase transition?[7] In this paper, we present a systematic study on ferroelectric and dielectric properties of the novel CBN TTB system with various x. Paraelectric-relaxor ferroelectric and incommensurate-commensurate phase transitions in CBN ceramics were analyzed by dielectric measurements. The grain growth could be governed by a mechanism of partial melting and nucleation.

II. EXPERIMENTAL PROCEDURE

A conventional mixed-oxide technique was used to prepare the samples with compositions $Ca_xBa_{1-x}Nb_2O_6$ ($x=0.22$, 0.30, and 0.38, denoted as CBN22, CBN30, and CBN38, respectively). The starting powders were reagent-grade $BaCO_3$, $CaCO_3$, and Nb_2O_5 as received. They were weighed and ball milled for 12 h with agate media in alcohol. Pellets of mixed powders pressed under a low pressure were calcined at 1150 °C for 2 h. The calcined pellets were crushed and ball milled with agate media in alcohol again. The dried powders were then compacted into pellets by a cold isostatic pressing. To get high density and observe the grain growth of the CBN ceramics, a two-step sintering method was employed. The pellets were first sintered in an alumina crucible at 1200 °C for 4 h and then sintered at 1250, 1300, and 1350 °C, respectively for 2 h. Samples for dielectric and ferroelectric measurements were electroded with a low-temperature-fired silver paint.

The structure of the ceramic samples was analyzed with x-ray diffraction (XRD) (X' Pert PRO MPD, Philips) using Cu $K\alpha$ ($\lambda=1.540\,56$ Å) radiation. Microstructure evolution was observed using a field emission scanning electron micro-

[a)]Electronic mail: keshanming@gmail.com.
[b)]Authors to whom correspondence should be addressed. Electronic addresses: hqfan3@163.com and aphhuang@polyu.edu.hk.

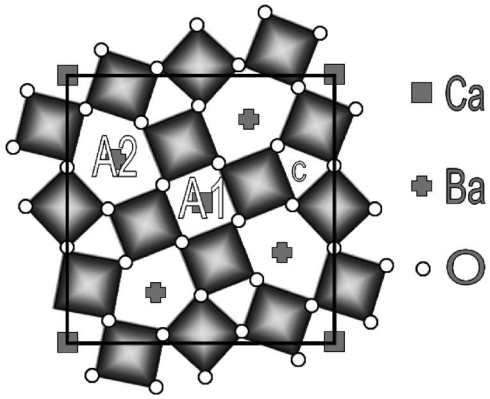

FIG. 1. The [001] projection of the TTB crystal structure of CBN (Ref. 10).

scope (FE-SEM) (JEOL Techniques) operated at 3 kV. Micro-Raman spectra measurements were performed on a JY HR800 Raman spectrometer under backscattering geometry. An argon ion laser was used as the excitation source with an output power of 15 mW at 488 nm.

Weak-field dielectric response was measured by a *LCR* meter (HP4194) with a four-wire probe and a signal level of 1 V/mm, in a frequency range of 1 kHz–1 MHz. Samples were measured during heating from room temperature to 500 °C and subsequently cooling down to room temperature again at a heating or cooling rate of 2 °C/min. Ferroelectric hysteresis loop (*P-E* loop) and time dependent leakage current were measured using a ferroelectric tester (RT66, Radiant Technology).

III. RESULTS AND DISCUSSIONS

A. Tetragonal tungsten bronze phase of CBN

The unit cell of a TTB structure can be derived by rotating and distorting 10 BO_6 octahedra. The rotations of the octahedra result in three types of interstitial positions, including 2 A1 voids, 4 A2 voids, and 4 C voids.[12] The A sites in SBN are partially filled, in which only five of the six A1 and A2 voids are occupied with strontium or barium cations while the smallest C voids are unoccupied.[12] Because of its smaller ionic radius, calcium can occupy A1 voids. Recently, atomic-resolution imaging of CBN using the negative Cs imaging (NCSI) technique[10] confirmed that CBN belongs to A-site filled TTB structure, as shown in Fig. 1. In CBN, calcium atoms occupy some of the A1 voids and barium atoms occupy the remaining A1 and A2 voids.

Figure 2 shows XRD patterns of the CBN synthesized at 1150 and 1350 °C respectively. The diffraction peaks in the XRD patterns can all be ascribed to the crystalline TTB phase, except for CBN38. Some unknown phases were observed for CBN38, as indicated by the asterisk in Fig. 2(a). The intensity of the strongest diffraction peak of the impurity phase is only 2.4% of that of the CBN phase. It means that the impurity phase should not significantly affect the properties of CBN ceramics. This result is slightly different from that reported by Ismailzade,[9] who claimed that a solid solution of $Ca_xBa_{1-x}Nb_2O_6$ can be formed with $x<0.4$, since the smaller Ca cations can only occupy A1 positions in the TTB structure.

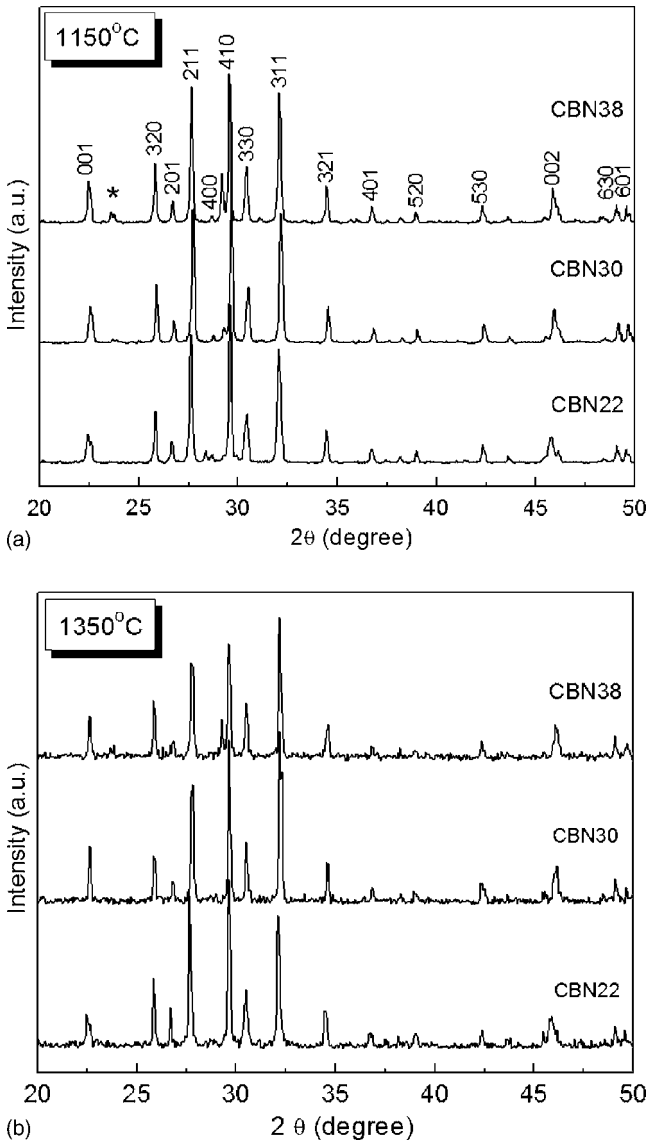

FIG. 2. XRD patterns of CBN ceramic powders synthesized at 1150 and 1350 °C, respectively.

It is known that SBN crystals have significant intrinsic disorders in atomic arrangements, giving relaxor-type phase transitions and broad Raman scattering spectra in these crystals.[13,14] The room-temperature micro-Raman spectra of the polished CBN ceramics prepared under different sintering temperatures are presented in Fig. 3. The micro-Raman spectra of $Sr_{0.4}Ba_{0.6}Nb_2O_6$ ceramics is also illustrated as a comparison. Spectra of CBN shown in Fig. 3 are similar to that of SBN single crystals[13] and ceramics (Fig. 3), indicating a phase transition behavior similar to that of SBN as discussed in next section. For CBN22, two broad and strong A_1(TO) phonon peaks at 260 and 640 cm^{-1}, which are related to ionic motions parallel to the *z*-axis and two weak peaks at 418 and 848 cm^{-1} are observed. The peak at 260 cm^{-1} is assigned to the deformation of O–Nb–O bond, and the peak at 640 cm^{-1} is due to the elongation of O–Nb bond, whereas the peak at 848 cm^{-1} is associated with the deformation of NbO_6 octahedron.[13,14] The very weak peak at 418 cm^{-1} is the A_1 mode of Nb–O elongation in CBN. The

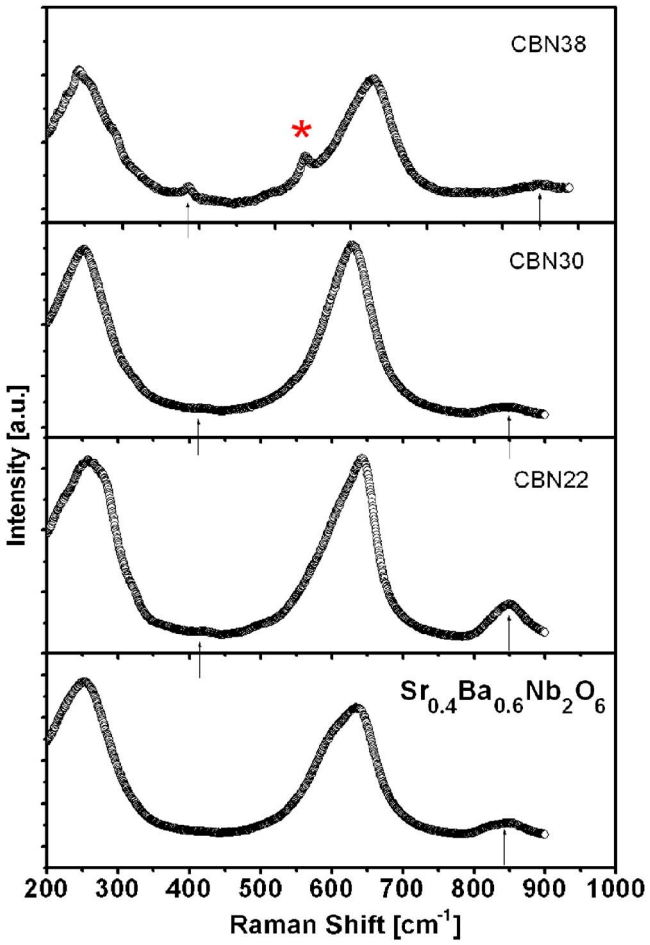

FIG. 3. (Color online) Micro-Raman scattering spectra for $Sr_{0.4}Ba_{0.6}Nb_2O_6$, CBN22, CBN30, and CBN38 samples.

bandwidth of the Raman peak increases with increasing Ca contents, which is accompanied by an increased disorder in TTB structure.

B. Phase transition of CBN

The complex dielectric permittivity, $\varepsilon=\varepsilon'-i\varepsilon''$, and loss tangent, $\tan\delta=\varepsilon''/\varepsilon'$, as a function of temperature at various measurement frequencies for CBN22, CBN30, and CBN38 sintered at 1350 °C for 2 h, are shown in Figs. 4–7. Two distinct relaxation features were observed in all three compositions. These dispersive phenomena were named as α and β, respectively. A very similar phenomenon has been observed in SBN system.[15] However, the two dielectric anomalies have not been clearly reported in CBN single crystals.[6–8]

In Fig. 4, a large drop in Curie temperature was observed when the composition was changed from CBN22 to CBN30, but only a small one was observed when the composition was further changed from CBN30 to CBN38. Considering that in solid solutions the transition temperature is generally linearly dependent on composition,[16] we can conclude that the solubility limit of the calcium content in CBN x should be slightly smaller than 0.38, as revealed by XRD in Fig. 2.

The α dielectric dispersion appeared near the Curie temperature range, which is attributed to the temperature and frequency dependencies of dielectric permittivity of relaxor

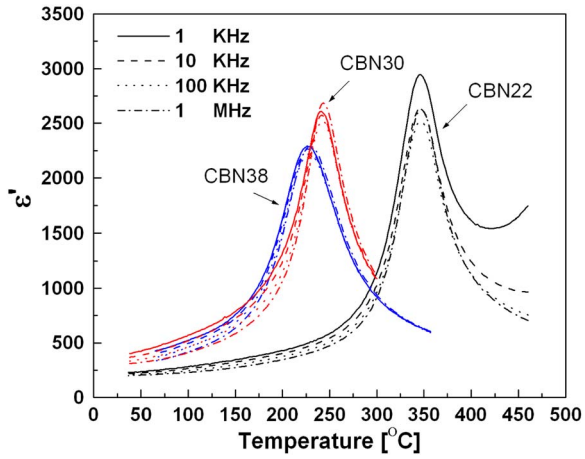

FIG. 4. (Color online) Frequency dependence of dielectric constant ε' as a function of temperature for CBN22, CBN30, and CBN38 ceramics sintered at 1350 °C.

ferroelectrics near the ferroelectric-paraelectric phase transition as their characteristics. With increasing calcium content, the dielectric dispersion is getting stronger, as shown in Figs. 5–7, reflecting an enhanced disorder. It should be noted that there exists another strong dielectric dispersion in the high temperature range (from 400 to 500 °C) for CBN22. A similar high temperature dispersion was observed in CBN28 single crystals,[7] which has been attributed to relaxor transition. However, we could not find the same phenomenon in CBN30 and CBN38 ceramics. With the highest Curie temperature, CBN22 has much higher concentration of polar nanoclusters than CBN30 and CBN38, which would offer a strong competitive effect with conduction process. The high temperature dielectric dispersion in CBN22 should result from the competitive effects induced by the dielectric relaxation and the disturbance of the electrical conduction, which has been reported in many other ferroelectric perovskites.[17,18]

The feature of β phase can be clearly seen in the temperature dependence of ε'' and tan δ, which showed a strong Debye-type dielectric dispersion. The α-β phase transition temperature also decreases with increasing calcium content, from 150 °C for CBN22 to 100 and 68 °C, for CBN30 and

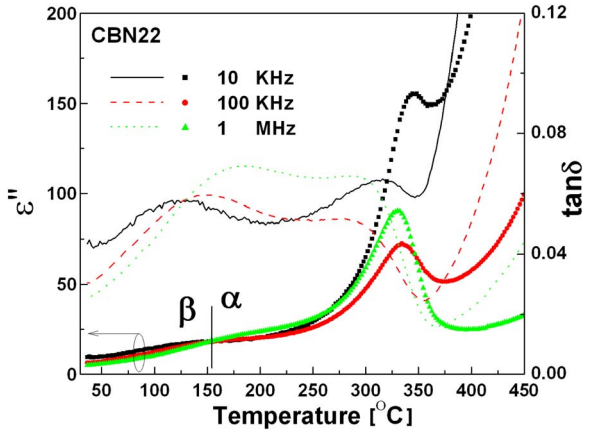

FIG. 5. (Color online) Temperature dependence of dielectric loss factor (ε'') and loss tangent (tan δ) of the CBN22 ceramics sintered at 1350 °C.

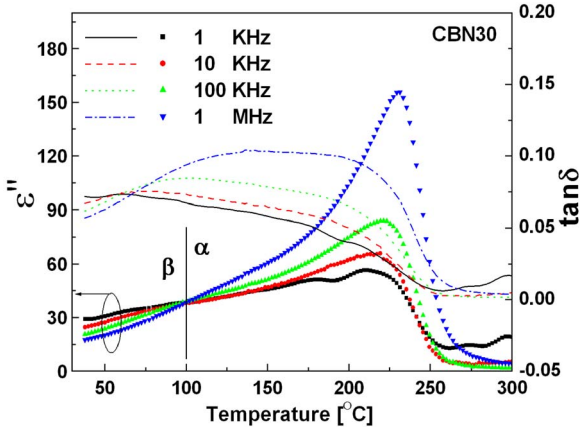

FIG. 6. (Color online) Temperature dependence of dielectric loss factor (ε'') and loss tangent (tan δ) of the CBN30 ceramics sintered at 1350 °C.

38, respectively. High-resolution transmission electron microscopy (HRTEM) evidence for an incommensurate-commensurate phase transition at around −75 °C in SBN50 single crystal was reported by Bursill and Lin,[19] corresponding to a β phase. Therefore, considering the similarity in dielectric properties of CBN and SBN, the β dielectric dispersion behavior of CBN might also be taken as an experimental evidence of the incommensurate superlattice structure. Recently, HRTEM investigation on CBN28 single crystals confirmed the existence of an incommensurate phase in CBN,[20] which was thought to be caused by the uniform mixing of slabs of two orthorhombic cells.[20]

C. Processing dependent properties of CBN

Figure 8 shows the temperature dependence of ε' and tan δ of CBN38 sintered at 1250, 1300, and 1350 °C, respectively. All these samples show the same phase transition behavior as discussed above. However, the Curie temperatures are 251, 243, and 232 °C, for the ceramics sintered at 1250, 1300, and 1350 °C, respectively. It is interesting to find that the sintering temperature has only a little effect on the dielectric constant of the paraelectric phase, but the dielectric constant of the ferroelectric phase is significantly increased with increasing sintering temperature. Around the β phase

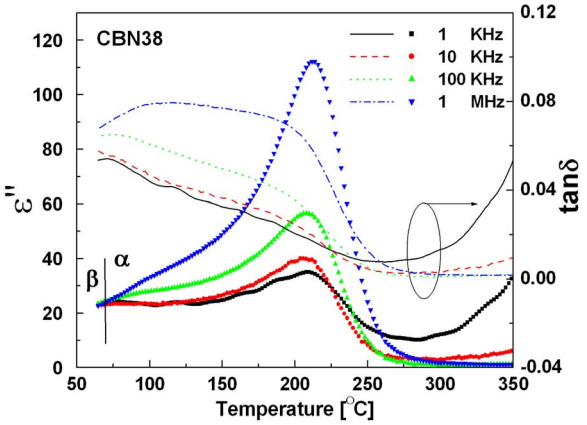

FIG. 7. (Color online) Temperature dependence of dielectric loss factor (ε'') and loss tangent (tan δ) of the CBN38 ceramics sintered at 1350 °C.

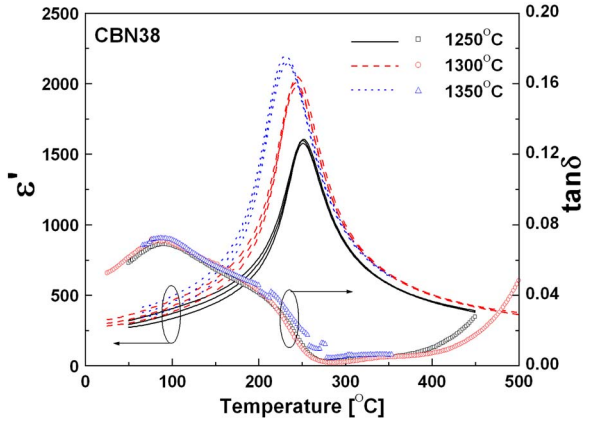

FIG. 8. (Color online) Temperature dependence of dielectric constant (ε') and loss tangent (tan δ) of the CBN38 ceramics sintered at 1250, 1300, and 1350 °C, respectively.

transition temperature, a dielectric loss peak is observed, which is Debye-type and related to the "lock in" of the incommensurate phase.[21]

Figure 9(a) shows the typical polarization-electric field

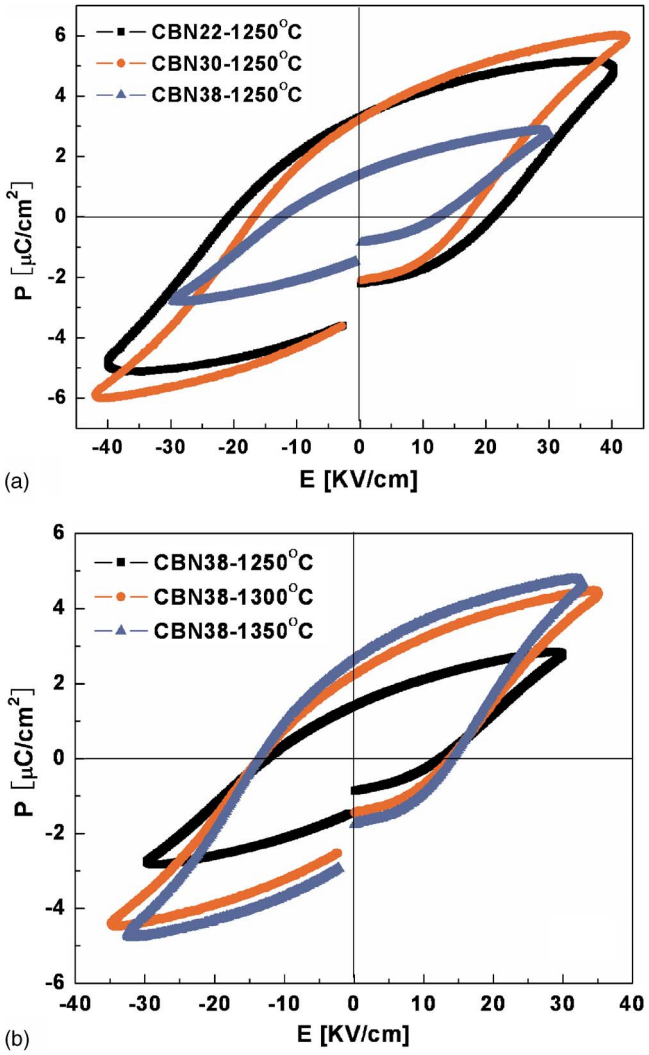

FIG. 9. (Color online) Ferroelectric hysteresis loop of (a) CBN22, CBN30, and CBN38 ceramics sintered at 1250 °C and of (b) CBN38 ceramics sintered at 1250, 1300, and 1350 °C.

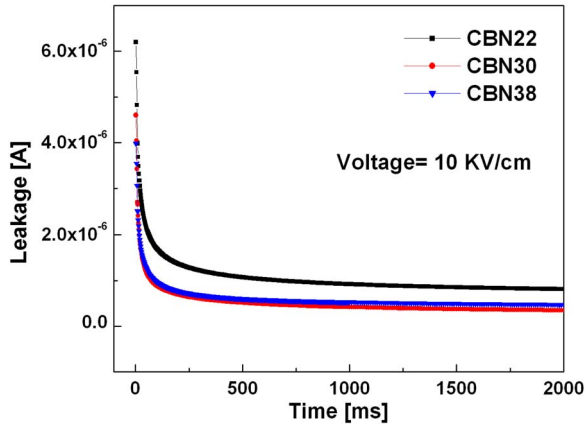

FIG. 10. (Color online) Leakage current vs time for CBN22, CBN30, and CBN38 ceramics sintered at 1250 °C under an applied dc electric field of 10 kV/cm.

(*P-E*) hysteresis loops for CBN22, CBN30, and CBN38 sintered at 1250 °C and Fig. 9(b) shows the *P-E* loops for CBN38 sintered at different temperatures. Smaller remnant polarizations P_r (all below 4 $\mu C/cm^2$, under an applied electric field 40 kV/cm) were observed in CBN ceramics than that of the [001]-oriented CBN single crystals (18 $\mu C/cm^2$, under an applied electric field of 60 kV/cm) reported.[6,7] Tetragonal CBN, such as SBN, exhibits only 180° domains because it undergoes a ferroelectric-to-paraelectric phase transition while retaining tetragonal.[22] The large difference in remnant polarization between ceramics and single crystals implies that the ferroelectric property of CBN is strongly orientation dependent. Furthermore, the orientation dependent dielectric properties of CBN28 single crystals have been reported by Song *et al.*[6]

Leakage current versus time of the CBN ceramics with different compositions under an applied dc field of 10 kV/cm is shown in Fig. 10. The leakage current decreases with time and then levels off to a constant value, which is the true leakage current. The decreasing trend of the leakage current at the initial stage results from the polarization current and charge trapping effects,[23] due to vacancies and defects in the ceramics. All the three samples show high resistivity and the leakage current increase with decreasing calcium content.

D. Grain growth of CBN

As mentioned above, the dielectric and ferroelectric properties of CBN ceramics are very sensitive to sintering temperatures. As a result, it is necessary to study its microstructure evolution. The FE-SEM micrographs of the three samples sintered at 1350 °C are presented in Fig. 11. All the grains show pillar-type morphology and the length of grains ranges from several to twenty micrometers. The growth direction of the pillar grains is their *c* axes, which was confirmed by electrical diffraction pattern.[24] At the end of the pillar grains, growth spirals can be observed in CBN22 and CBN30 [Figs. 11(a) and 11(b)] which resemble that observed in single crystals. The absence of growth spirals in CBN38 [Fig. 11(d)] also gives a conclusion that the grains of CBN38 can fully grow at 1350 °C, and the optimal sintering temperature of CBN22 and CBN30 should be higher. Figure 11(c) shows a fracture surface of CBN30. Transgranular fracture mode of CBN ceramics could be observed.

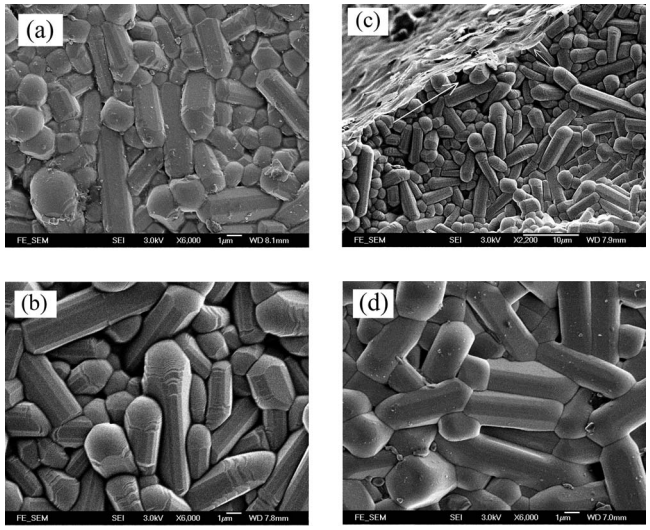

FIG. 11. SEM images of (a) CBN22, (b) CBN30, and (d) CBN38 ceramics sintered at 1350 °C. (c) The SEM image of the fracture surface of CBN30 ceramics.

It is known that spiral growth usually takes place during solution growth or melt growth of single crystal materials.[25] This is a grain growth mechanism that is related to the packing atoms on steps of a screw dislocation. Figure 12 shows the surface morphology of CBN38 sintered at different temperatures. Mass transport for such a step process cannot be accounted for the usual mechanism of sintering by fusion of adjacent grains. There should be an initial partial melting of the grains where the nucleation occurs as arrowed in Fig. 12(b). Consequently, mass transport necessary for this process takes place by the diffusion of ions to the growing steps through the fluid phase that might prevail in the partial liquid conditions.[26,27] At a lower sintering temperature, this process needs a much longer time to grow fully [Figs. 12(a)–12(c)], while it grows quickly at a higher sintering temperature [Fig.

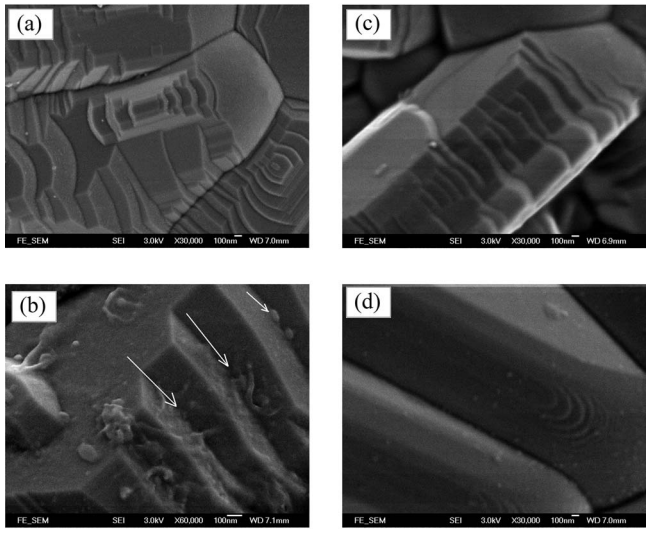

FIG. 12. SEM images of the CBN38 ceramics sintered at [(a) and (b)] 1250 °C, (c) 1300 °C, and (d) 1350 °C.

12(d)]. This explains satisfactory the observation of the growth spirals at the ends of the rods. Meanwhile, the different grain size and grain boundary morphology introduce a processing-dependent dielectric and ferroelectric properties of the CBN ceramics as discussed above.

IV. CONCLUSION

Partially filled $Ca_xBa_{1-x}Nb_2O_6$ tungsten bronze ceramics were prepared by a two-step sintering strategy, and their dielectric characteristics were investigated together with their phase transition features. All ceramics (CBN22, CBN30, and CBN38) show a phase transition from a diffused α phase to an incommensurate β lock in phase above room temperature. The dielectric and ferroelectric properties of the CBN ceramics were very sensitive to the final sintering temperature. Growth spirals at the ends of the pillar grains were observed which may be due to a partial melting and nucleation mechanism.

ACKNOWLEDGMENTS

This work was supported by the National Nature Science Foundation (No. 50672075), the RFDP (No. 20050699011) and 111 project (No. B08040) of MOE, and the Aeronautic Science Foundation (No. 2006ZF53068) of China, as well as the Research Grants Council of the Hong Kong Special Administrative Region, China (Project No. PolyU5166/05E).

[1]P. V. Lenzo, E. G. Spencer, and A. A. Ballman, Appl. Phys. Lett. **11**, 23 (1967).
[2]A. S. Bhalla, R. Guo, G. Burns, F. Dacol, and R. R. Neurgaonkar, Phys. Rev. B **36**, 2030 (1987).
[3]S. M. Ke, H. T. Huang, H. Q. Fan, H. L. W. Chan, and L. M. Zhou, J. Phys. D: Appl. Phys. **40**, 6797 (2007).
[4]M. Eßer, M. Burianek, D. Klimm, and M. Muhlberg, J. Cryst. Growth **240**, 1 (2002).
[5]H. L. Song, H. J. Zhang, X. G. Xu, X. B. Hu, X. F. Cheng, J. Y. Wang, and M. H. Jiang, Mater. Res. Bull. **40**, 643 (2005).
[6]H. L. Song, H. J. Zhang, Q. Z. Jiang, X. G. Xu, C. J. Lu, X. B. Hu, J. Y. Wang, and M. H. Jiang, J. Cryst. Growth **290**, 431 (2006).
[7]Y. J. Qi, C. J. Lu, J. Zhu, X. B. Chen, H. L. Song, H. J. Zhang, and X. G. Xu, Appl. Phys. Lett. **87**, 082904 (2005).
[8]M. Eßer, M. Burianek, P. Held, J. Stade, S. Bulut, C. Wickleder, and M. Muhlberg, Cryst. Res. Technol. **38**, 457 (2003).
[9]I. G. Ismailzade, Kristallografiya **5**, 268 (1960).
[10]C. L. Jia, J. Schubert, T. Heeg, S. B. Mi, H. Y. Chen, B. Joschko, M. Burianek, M. Muhlberg, and K. Urban, Acta Mater. **54**, 2383 (2006).
[11]S. B. Mi, C. L. Jia, K. Urban, T. Heeg, and J. Schubert, J. Cryst. Growth **291**, 243 (2006).
[12]W. L. Zhong, *Physics of Ferroelectrics* (Science Press of China, Beijing, 1996).
[13]K. G. Bartlett and L. S. Wall, J. Appl. Phys. **44**, 5192 (1973).
[14]S. G. Lu, C. L. Mark, and K. H. Wong, J. Am. Ceram. Soc. **86**, 1333 (2003).
[15]H. Q. Fan, L. Y. Zhang, and X. Yao, J. Am. Ceram. Soc. **33**, 895 (1998).
[16]J.-H. Jeon, J. Eur. Ceram. Soc. **24**, 1045 (2004).
[17]B. S. Kang and S. K. Choi, Appl. Phys. Lett. **80**, 103 (2002).
[18]B. S. Kang, S. K. Choi, and C. H. Park, J. Appl. Phys. **94**, 1904 (2003).
[19]L. A. Bursill and P. J. Lin, Philos. Mag. B **54**, 157 (1986).
[20]C. J. Lu, Y. J. Qi, J. Q. Li, H. J. Zhang, and J. Y. Wang, Appl. Phys. Lett. **89**, 191901 (2006).
[21]R. Blinc and A. P. Levanyuk, *Incommensurate Phases in Dielectrics* (North-Holland, Amsterdan, 1986), Vol. 1.
[22]C. J. Lu, C. J. Nie, X. F. Duan, J. Q. Li, H. J. Zhang, and J. Y. Wang, Appl. Phys. Lett. **88**, 201906 (2006).
[23]H. M. Chen, J. M. Lan, J. L. Chen, and J. Y. Lee, Appl. Phys. Lett. **69**, 1713 (1996).
[24]W. Chen, S. Kume, C. Duran, and K. Watari, J. Eur. Ceram. Soc. **26**, 647 (2006).
[25]C. H. L. Goodman, *Crystal Growth Theory and Techniques* (Plenum, London, 1974).
[26]H. Y. Lee and R. Freer, J. Appl. Phys. **81**, 376 (1997).
[27]H. Y. Lee and R. Freer, J. Mater. Sci. **33**, 1703 (1998).